Europium-doped calcium pyrophosphates: Allotropic forms and photoluminescent properties

A. Doat[a], F. Pellé[b] and A. Lebugle[a]

[a]CIRIMAT UMR CNRS 5085, Physico-Chimie des Phosphates, ENSIACET-INPT, National Polytechnic Institute of Toulouse, 118 route de Narbonne, 31077 Toulouse Cedex 4, France

[b]Laboratoire de Chimie Appliquée de l'Etat Solide, CNRS-UMR 7574 Chimie de la Matière Condensée de Paris, ENSCP, 11 Rue Pierre et Marie Curie, 75231 Paris Cedex 5, France

Abstract

In a search for new luminescent biological probes, we synthesized calcium pyrophosphates doped with europium up to an atomic Eu/(Eu+Ca) ratio of 2%. They were prepared by coprecipitating a mixture of calcium and europium salts with phosphate. After heating at 900 °C in air, two phases coexisted, identified as the β calcium pyrophosphate form and $EuPO_4$. Heating near 1250 °C in air, during the $\beta \rightarrow *$ transformation, europium ions substitute for calcium ions in the * calcium pyrophosphate structure as demonstrated by the spectroscopic study. Europium ions with both valence states (divalent and trivalent) were observed in the samples. Following the synthesis procedure, partial reduction of Eu^{3+} took place even in an oxidizing atmosphere. The 0.5%-doped compound could serve as a sensitive probe in biological applications. Depending on the excitation wavelength, the luminescence occurs either in the red or in the blue regions, which discriminates it from parasitic signals arising from other dyes or organelles in live cells.

Graphical abstract

Eu-doped * calcium pyrophosphate: an intrinsic biphotonic probe for biology: (a) Eu^{3+}; (b) Eu^{2+}.

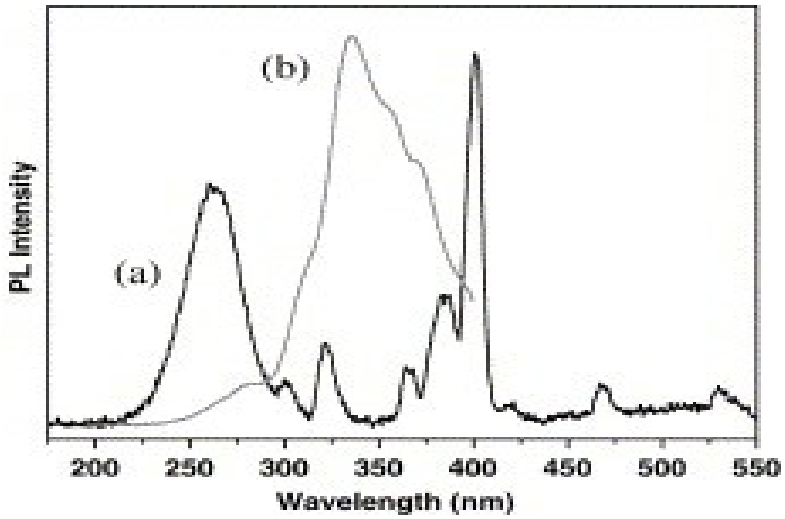

Keywords: Calcium pyrophosphate; Eu^{2+}; Eu^{3+}; Luminescence

1. Introduction

We have recently demonstrated that nanoparticles of biomimetic calcium phosphates with apatitic structure, doped with europium, can be used as luminescent biological probes. Internalization of such probes by living cells was followed by monitoring the europium fluorescence [1]. Among the various calcium phosphates, others with a different composition or structure might also find applications in this field, due to their improved optical or biological characteristics compared to that of the previously studied probes [1]. Calcium pyrophosphates constitute a wide family, which, to our knowledge, has been little explored, although their biocompatibility is well established [2].

Few studies on europium-doped pyrophosphates have been reported in the literature. Most of them concern pyrophosphates doped with divalent europium ions, whose luminescence occurs in the blue range. Wanmaker and Vrugt [3] obtained europium-doped $*$ calcium pyrophosphate by a solid-state process, at 1200 °C, but under reducing atmosphere. The synthesis was carried out mainly by a solid-state reaction between monetite $CaHPO_4$, diammonium hydrogen phosphate and europium oxide. Slightly reducing conditions (0.1–2% hydrogen) afforded a Eu^{2+}-doped compound.

Nazarova [4] has indicated the possibility of synthesizing calcium or strontium pyrophosphate doped with Eu^{2+} under air atmosphere and at high temperature, but did not provide any details on the experimental conditions.

Few studies have been devoted to pyrophosphates doped with trivalent europium. Pelova and Grigorov [5] reported the synthesis of europium-doped zirconium pyrophosphate (ZrP_2O_7:Eu) under air atmosphere and at high temperature. After heating at 900 °C, only Eu^{3+} ions were observed in zirconium pyrophosphate, whereas after heating at 1100 °C, Eu^{2+} ions were detected. The reduction from Eu^{3+} to Eu^{2+} ions thus occurred in zirconium pyrophosphate at high

temperature, even under air atmosphere. The transformation became total only under slightly reducing atmosphere.

Such abnormal partial reduction of Eu^{3+} at high temperature under non-reducing atmosphere has also been described by Chinese workers [6], [7], [8], [9], [10] and [11] in the case of borates and aluminates. Thus, Zeng et al. [6] reported that reduction of Eu^{3+} to Eu^{2+} only occurred in SrB_6O_{10}:Eu by heating under air atmosphere. In a similar way, Pei et al. [7] and [8] observed the reduction of Eu^{3+} to Eu^{2+} in $Sr_2B_5O_9Cl$:Eu and SrB_4O_7:Eu by heating at high temperature (900 °C) under air. Peng et al. [9] also observed this reduction by heating at 1400 °C under air in $Sr_4Al_{14}O_{25}$:Eu. Su et al. [10] and Liang et al. [11] obtained the same reduction by heating at 1000 °C under air in $SrBPO_5$:Eu and $CaBPO_5$:Eu. However, this reduction has not been reported in the case of calcium pyrophosphate.

We investigated here the doping of a calcium pyrophosphate [$Ca_2P_2O_7$] by europium ions and the influence of this doping on the phases obtained and luminescence spectra recorded. Dicalcium phosphate dihydrate [$CaHPO_4{\cdot}2H_2O$] (DCPD) samples synthesized in the presence of europium ions were heated in air at temperatures where the β and $*$ forms of calcium pyrophosphates are stable. The different phases present in the heated samples were identified and related to the luminescence spectra observed. Special attention was given to the oxidation state (II or III) of europium ions. These results further the understanding of europium doping in calcium pyrophosphate.

2. Materials and methods

2.1. Synthesis

Europium-doped calcium pyrophosphates were obtained by gradually heating DCPD in the presence of europium ions at different temperatures. DCPD was synthesized at room temperature by double decomposition of ammonium phosphate and calcium nitrate. In order to obtain DCPD in which europium is intimately mixed, europium ions were added to the calcium solution at an atomic ratio $R_L = Eu/(Eu+Ca)$ between 0% and 2%, and the synthesis was carried out in a similar way.

Solution A contained a total of 70.6 mmol of calcium nitrate [$Ca(NO_3)_2{\cdot}4H_2O$] (Carlo Erba) and europium nitrate [$Eu(NO_3)_3{\cdot}6H_2O$] (Alfa Aesar) in appropriate proportions, dissolved in 100 mL of deionized water. Solution B contained 62.7 mmol of ammonium dihydrogen phosphate [$(NH_4)H_2PO_4$] (Carlo Erba) dissolved in 208 mL of deionized water and 4.2 mL of ammonia (11 M). Solution A was rapidly added to solution B at room temperature while stirring. After 5 min stirring, the precipitate was quickly filtered and washed successively with 167 mL of deionized water and 50 mL of ethanol. The gel obtained was freeze-dried.

In order to obtain β pyrophosphate, samples were progressively heated (4°/min) to 900 °C and left for 1 h at this temperature. All the heat treatments were carried out under air.

To obtain $*$ pyrophosphate, the previous samples were further heated at 1250 °C for 15 min under air, and then quenched in liquid nitrogen. In some cases, they were heated at 1275 °C for 30 min.

$Ca_3Eu(PO_4)_3$ was also synthesized using the method described by McCarthy [12]. After quenching in liquid nitrogen, the product was analyzed by X-ray diffraction (XRD) (JCPDS No. 29-321). This compound was prepared for the spectroscopic analysis to interpret the results, as described below.

2.2. Chemical analysis

Europium ion content was determined by Induced Coupled Plasma Atomic Emission Spectroscopy analysis (ICPAES) at the Service Central d'Analyse of the CNRS (Vernaison, France) (relative error: 3%). Calcium and europium ions were assayed together by volumetric titration [13] (relative error: 0.5%).

Orthophosphate ions were determined by colorimetry as phosphovanadomolybdenum ($l = 460\ \mathrm{nm}$) (relative error: 0.5%). The (Ca+Eu)/P atomic ratio had a relative error of 1%.

2.3. X-ray diffraction (XRD)

XRD patterns were obtained with a CPS 120 INEL diffractometer using the $K*1$ radiation of a cobalt anticathode ($\lambda = 1.78892\ \mathrm{\AA}$).

2.4. Scanning electron microscopy (SEM) and energy dispersive analysis of X-rays (EDAX)

The powders were observed with a LEO 435 VP electron microscope. After deposition on an adhesive coating pasted on sample holder, the samples were metallized with silver during 1 min to prevent build-up of surface charge. Observations were carried out either by secondary electron detection, or by retro-diffused electron detection. The brightness produced by the latter increases with atomic number of the atoms. Europium-rich areas (high Z) can be differentiated by their clear appearance. EDAX was also carried out with the same apparatus.

2.5. Luminescence

UV excitation was provided either by a high-pressure mercury lamp equipped with a Wood filter or by a XBO 150 xenon lamp with wavelength selection using a HD20 Jobin-Yvon monochromator. The selective excitation was provided by a tunable frequency dye laser (Coherent 599) pumped by a CW argon laser (Coherent Innova 300), Rhodamine 6G was used as laser dye. The fluorescence was dispersed through a HR1000 Jobin-Yvon monochromator equipped with a 1200 grooves mm^{-1} diffraction grating. The signal was detected by a RTC 56 TVP photomultiplier and amplified by a PAR 128a lock-in-amplifier with data acquisition on microcomputer. Appropriate filters were set in front of the spectrometer to eliminate parasitic signals from the excitation beam. All spectra were corrected for the response of the experimental set-up and filters.

3. Results

The composition of the samples before the heating steps was determined. Chemical analysis gave a (Ca+Eu)/P atomic ratio close to unity. Moreover, the Eu/(Eu+Ca) atomic ratio was in agreement with the theoretical atomic ratio R_L, used in the synthesis.

The samples heated at 900 and at 1250 or 1270 °C were investigated in more detail.

3.1. Samples heated in the stability range of β calcium pyrophosphate, at 900 °C

The XRD patterns of the samples with 0% and 2% atomic Eu/(Eu+Ca) ratio, heated at 900 °C, were recorded (Fig. 1). For the undoped material (R_L=0), all the observed reflection peaks corresponded to those of the β pyrophosphate $Ca_2P_2O_7$ phase (JCPDS No. 33-297 [14]). Doping with europium ions (R_L=2%) modified the XRD patterns, with additional reflections, and alterations in intensity of

some calcium pyrophosphate peaks. A shoulder at 37.1° appeared, the intensity of the (202) reflection of the β pyrophosphate, observed at 32.3°, increased, and a low-intensity peak was detected at 55.5°. They correspond, respectively, to the (012), (200) and (212) reflections of europium phosphate $EuPO_4$ (JCPDS No. 25-1055) whose strongest reflection ($(\bar{1}20)$, d=3.03) is hidden by the (008) peak of the β pyrophosphate at 34.5°. Moreover, a shoulder at 36.1°, and another low-intensity peak at 40.1° were also observed, attributed to the (0210) and (220) peaks of β tricalcium phosphate $Ca_3(PO_4)_2$ (β TCP).

Fig. 1. X-ray diffraction patterns of the samples heated at 900 °C, with R_L=0% (a) and R_L=2% (b).

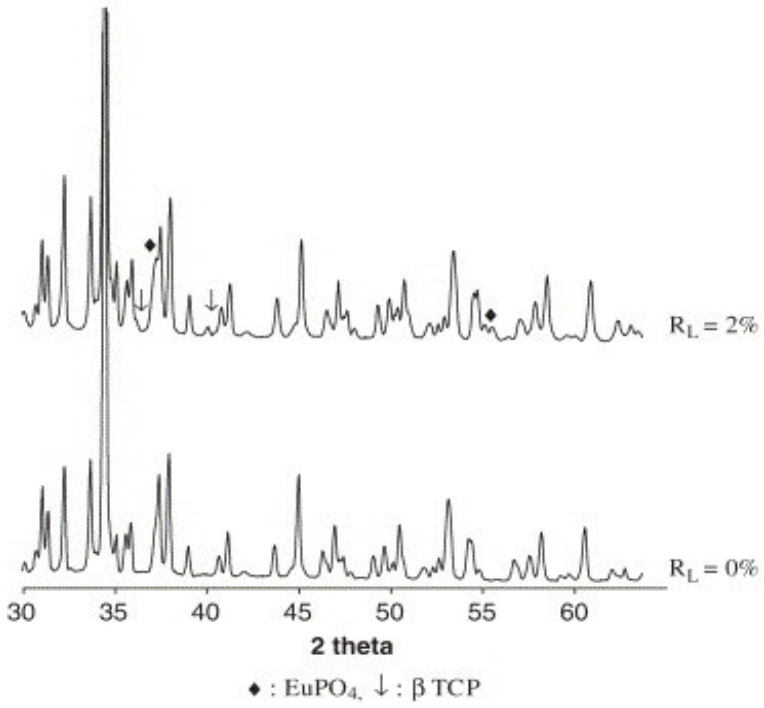

The samples were observed by SEM. The β pyrophosphate phase, with R_L=0%, appeared as large thin sheets (5–8 μm long) (Fig. 2(a)). The sample doped with 2% europium was observed by retro-diffused electron detection (Fig. 2(b)). A second phase in low proportion was seen as a clearer shade than the main β pyrophosphate phase, indicating the presence of europium in higher concentration, which was supported by the EDAX analysis. The EDAX spectrum of this second phase (Fig. 3(b)), indicated a high concentration of europium, whereas the main phase lacked europium (Fig. 3(a)).

Fig. 2. SEM picture of the samples heated at 900 °C, with R_L=0% (a) and 2% (b) (retro-diffused electron detection).

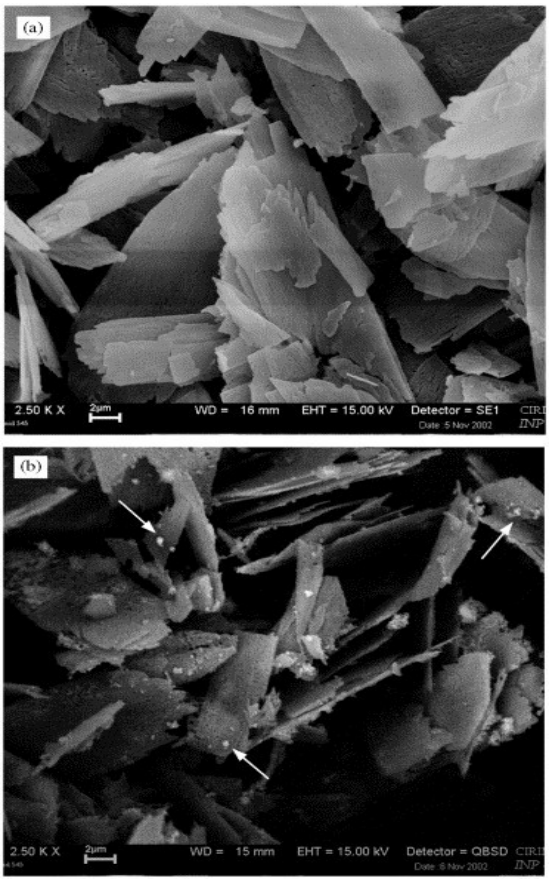

Fig. 3. EDAX spectra of the sample heated at 900 °C, with R_L=2%, carried out on the main phase (a) and on the minor phase (b).

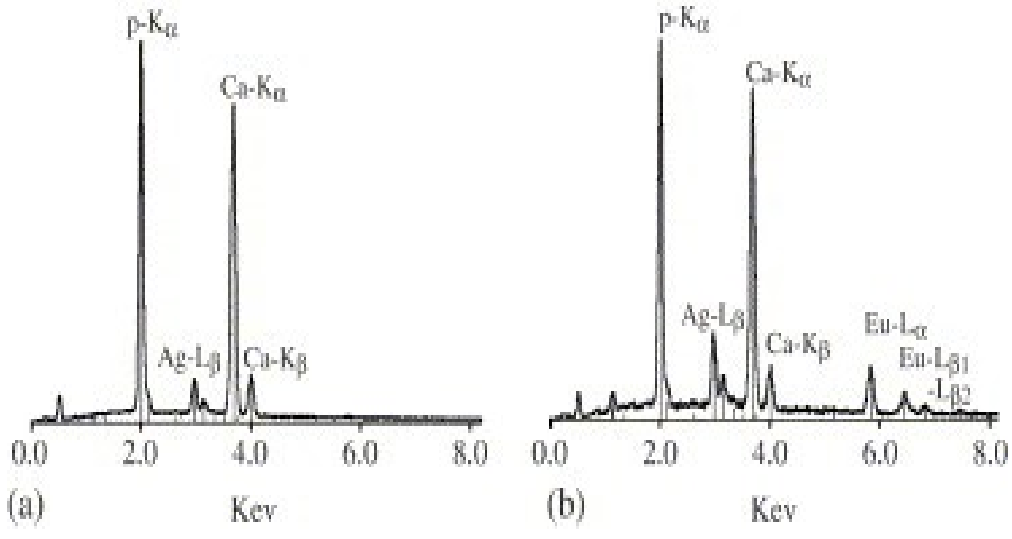

The luminescence excited in the UV at 253.7 nm or in the visible with the Argon laser line at 465.8 nm enabled observation of narrow spectral features in the visible range of the spectrum, between 570 and 720 nm, corresponding to electronic transitions within the $4f^6$ configuration of Eu^{3+} ions (Fig. 4). The emission spectrum is dominated by the $^5D_0 \rightarrow {}^7F_2$ hypersensitive transition. Upon excitation at 253.7 nm (Fig. 4(a)), the relative intensities of the different transitions and the energy of the different components resembled those of pure $EuPO_4$ [15]. This is in agreement with the results obtained by XRD. However, on excitation at 465.8 nm, extra emission lines were observed (Fig. 4(b)). Most of these lines matched those in the spectrum of europium-doped β tricalcium phosphate reported by Lazoriak et al. [16].

Fig. 4. Luminescence emission spectrum of the sample heated at 900 °C, with R_L=2%: (a) excitation at 253.7 nm, (b) excitation at 465.8 nm.

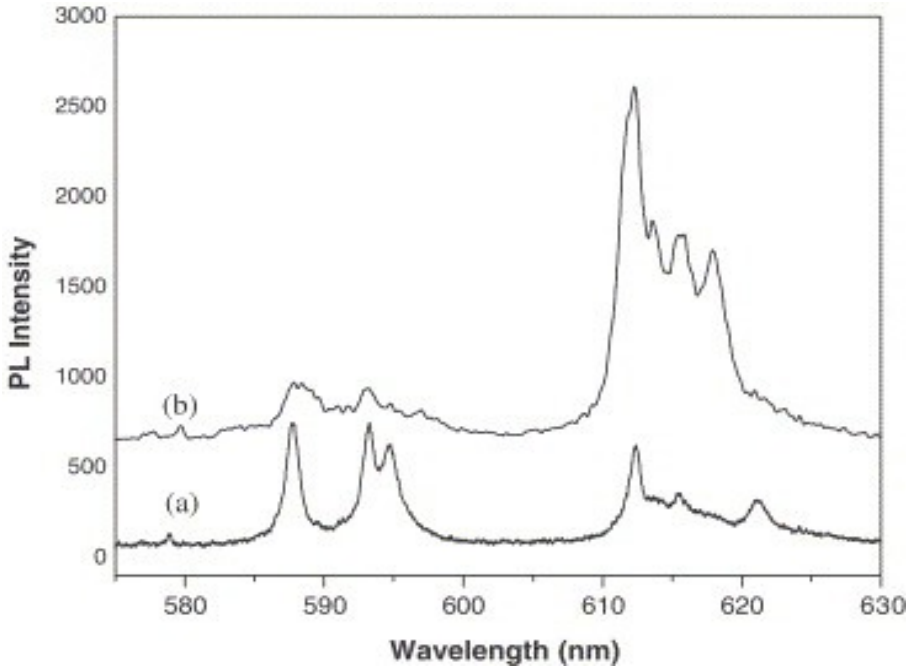

From these data, the minor phases identified as $EuPO_4$ and/or Eu-doped $Ca_3(PO_4)_2$ probably corresponded to the small europium-rich balls observed by SEM at the surface of the crystal. The optical data indicated that the europium ions were all in the trivalent state in this sample.

3.2. Samples heated in the stability range of ∗ calcium pyrophosphate, at 1250–1270 °C

3.2.1. Samples heated at 1250 °C

The XRD patterns recorded for the samples doped with 0% and 2% Eu/(Eu+Ca) atomic ratio, heated at 1250 °C, are represented in Fig. 5a and b. For the undoped sample (R_L=0), only the peaks of ∗ pyrophosphate $Ca_2P_2O_7$ were observed. After introduction of europium ions (R_L=2), apart from the main pyrophosphate phase, additional low-intensity peaks were observed. Most of them

were characteristic of europium phosphate $EuPO_4$ as previously described. Another diffraction peak was observed at 36.2°, as well as an increase in the (002) reflection intensity of $*$ pyrophosphate, observed at 40.1°. These results were ascribed to the presence of β tricalcium phosphate $Ca_3(PO_4)_2$ whose other main reflection (214) is superimposed on the (211) reflection of $*$ pyrophosphate at 32.4°.

Fig. 5. X-ray diffraction patterns of the samples heated at 1250 °C, with R_L=0% (a) and R_L=2% (b); at 1270 °C during 15 min, with R_L=2% (f); at 1270 °C during 30 min with R_L=2% (e), 1% (d) and 0.5% (c).

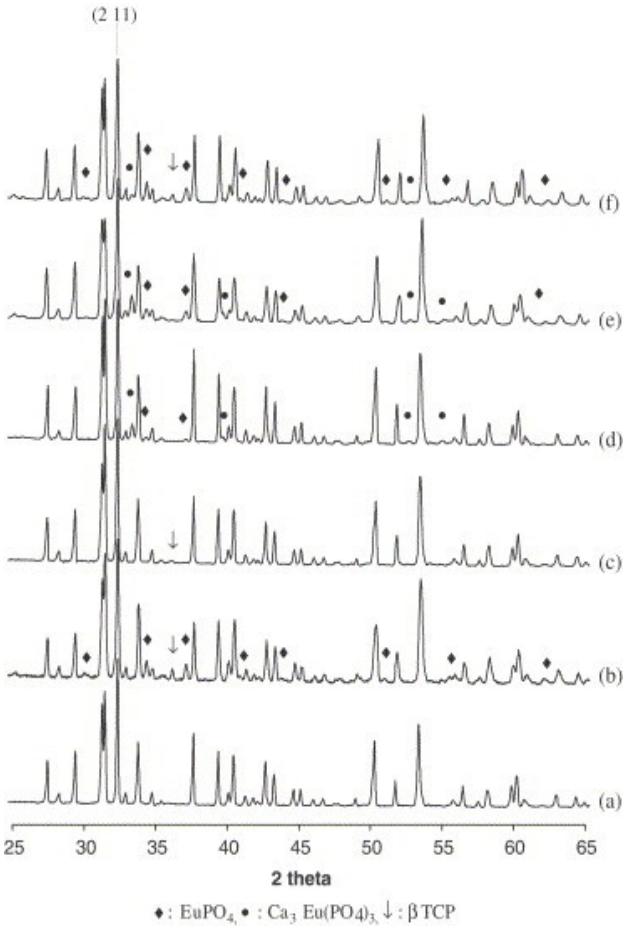

SEM observations of these samples showed that the crystallites were sintering. The sample with R_L=2% was observed by retro-diffused electron detection (Fig. 6). A white phase is clearly visible in Fig. 6 in addition to the main grey phase, indicating the presence of europium in higher proportion, supported by the EDAX analysis. This minor phase was attributed to phosphate rich in europium.

Fig. 6. SEM picture (retro-diffused electron detection) of the sample heated at 1250 °C, with R_L=2%.

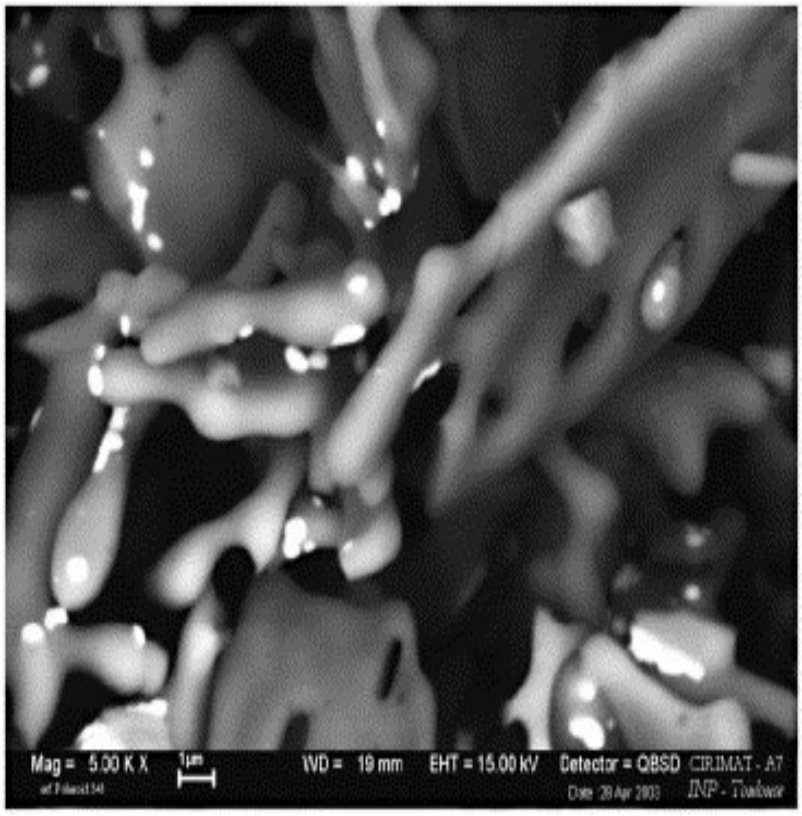

Luminescence study of the sample containing europium (2 at%), after heating at 1250 °C was investigated. The fluorescence emission spectrum recorded at 300 K under non-selective excitation at 253.7 nm is represented in Fig. 7. A wide dissymmetric band was observed peaking at 415 nm which was ascribed to the allowed transition from the lowest component of the $4f^6 5d^1$ configuration to the fundamental state $^8S_{7/2}$ of the $4f^7$ configuration of the Eu^{2+} ions. This oxidation state of europium ions was indicated by the EPR data. The presence of Eu^{2+} ions in a sample synthesized at high temperature and under non-reducing atmosphere (air) is of note. Narrow emission lines due to the $^5D_0 \rightarrow {}^7F_J$ (J=0,1,2,3,4) transitions of Eu^{3+} ions were also observed, ascribed to Eu^{3+} ions in the $EuPO_4$ phase. However, in this case, excitation using the argon laser line at 465.8 nm produced a more complex emission spectrum revealing the presence of Eu^{3+} in other positions in addition to that of the $EuPO_4$ ones (Fig. 8). The energies and the relative intensities of the additional lines corresponded to those reported by Lazoriak in europium-doped tricalcium phosphate [16]. The presence of two different phases identified by spectroscopy is in agreement with the XRD findings. Another peak of low intensity at 610.4 nm on both spectra should be noted. It will be assigned below.

Fig. 7. Luminescence spectra of the samples recorded under UV excitation at 253.7 nm. Sample heated at 1250 °C (a) 2% Eu, samples heated at 1270 °C (b) 2% Eu; (c) 1% Eu; (d) 0.5% Eu.

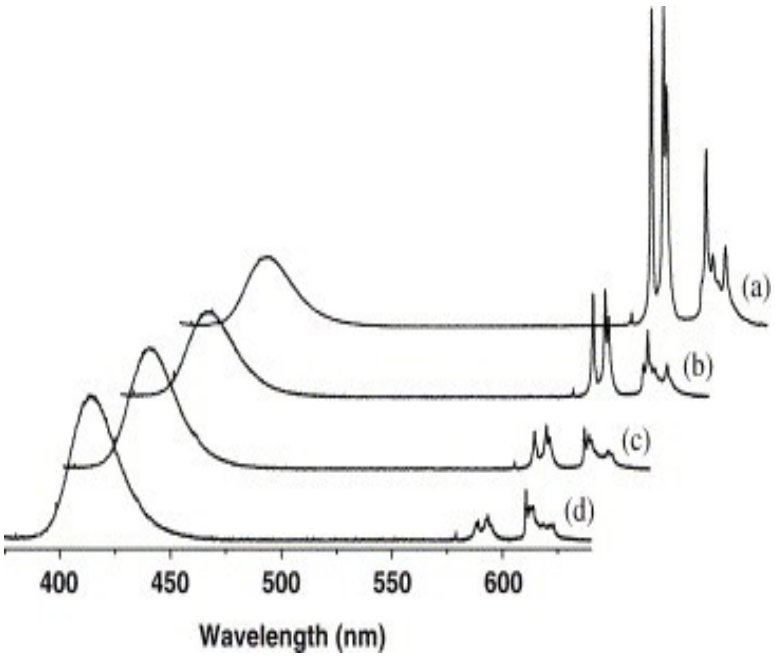

Fig. 8. Luminescence spectrum excited in the visible (465.8 nm) for samples heated at 1270 °C ((a) R_L=0.5%, (b) R_L=1%, (c) R_L=2%,) in comparison to that obtained for $Ca_3Eu(PO_4)_3$, curve (d).

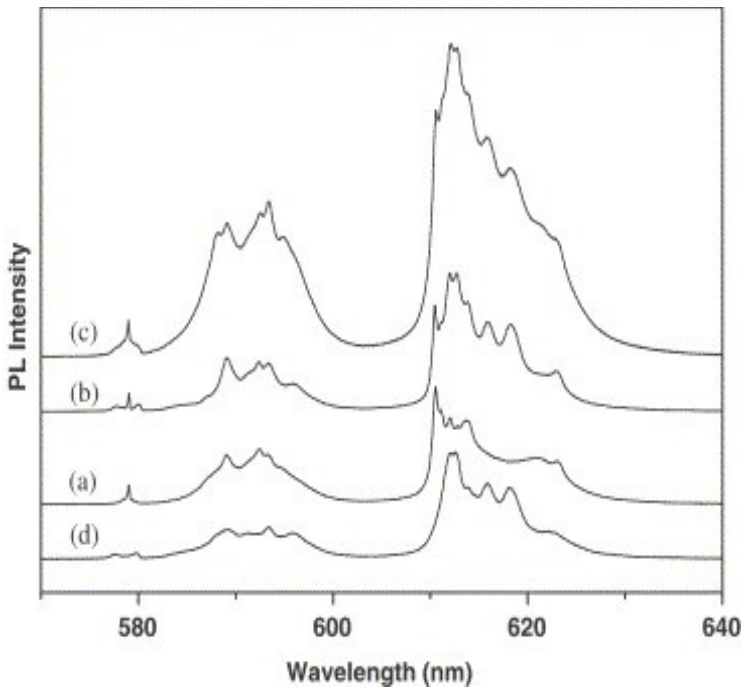

Furthermore, the influence of the heat treatment and its duration and of the europium concentration

on the structure of the samples was investigated.

3.2.2. Influence of the heat treatment

The influence of the heat treatment was investigated by heating the sample doped with 2% europium at 1270 °C instead of 1250 °C during 15 min. Additional peaks apart from the * pyrophosphate ones were detected by XRD (Fig. 5). In common with the sample heated at 1250 °C, they could be assigned to europium phosphate $EuPO_4$ and the βTCP phase. However, additional diffraction peaks were recorded and identified as a mixed phosphate $Ca_3Eu(PO_4)_3$ (JCPDS No. 29-321) of eulytite structure. The appearance of this phase at this temperature is in agreement with the results of the study of $Ca_3Ln(PO_4)_3$ (Ln=La–Gd) phases with eulytite structure reported by McCarthy et al. [12]. $Ca_3Ln(PO_4)_3$ was found to decompose below 1250 °C into $Ca_3(PO_4)_2$ and $LnPO_4$ (monazite). It is stable at the higher temperature and needs to be quenched in order to be observed.

Luminescence of the sample doped with Eu (2 at%) was dominated by an emission band peaking at 450 nm, ascribed to Eu^{2+} ions. On increasing the temperature, the Eu^{2+} emission intensity increased compared to that ascribed to Eu^{3+} ions (Fig. 7). This was indicative of an increasing concentration of reduced Eu^{2+} ions in the samples on increase in temperature of the heat treatment.

The influence of the duration of heating was studied on the sample with R_L=2%. The sample was heated at 1270 °C during 30 min instead of 15 min. XR Diffraction showed a progressive disappearance of the β TCP phase, a decrease in amount of $EuPO_4$, accompanied by an increase in $Ca_3Eu(PO_4)_3$ (Fig. 5).

3.2.3. Effect of doping with europium ions

The influence of the europium content was studied on samples heated for 30 min at 1270 °C. The XRD patterns of the different compounds with R_L=0.5%, 1% and 2% were recorded (Fig. 5). As noted previously, additional phases appeared next to * pyrophosphate. A low-intensity peak at 36.2° was detected with 0.5% europium. From the previous results, it was attributed to β TCP. $EuPO_4$ and $Ca_3Eu(PO_4)_3$ were detected with increase in europium concentration.

In addition, the half-width at half-maximum (HWHM) of the (211) of the * pyrophosphate reflection peak was measured as a function of the europium concentration. It increased markedly with R_L up to R_L=0.5% (from $2.2.10^{-3}$ to $2.7.10^{-3}$ rad), and then exhibited a weak dependence on R_L up to 2% ($2.8.10^{-3}$ rad). The increase observed between 0% and 0.5%, reflects either a reduction in size of the crystallites or a crystallinity with europium in the lattice. This suggests that europium is in the * pyrophosphate structure. The slower evolution of the HWHM with increasing europium concentration for R_L>0.5% was attributed to a substitution limit of europium in that structure.

On UV excitation (253.7 nm), the luminescence spectrum showed, at all europium concentrations, a wide dissymmetric band peaking at 415 nm as well as narrow emission lines between 570 and 720 nm as observed for samples heated at 1250 °C (Fig. 7). The relative intensities of the wide band and narrow lines were a function of the Eu^{3+} concentration in the samples. For the lowest concentration, the fluorescence spectrum was dominated by the wide band peaking at 415 nm. On increase in the europium content, narrow lines observed in the visible region became the most intense (Fig. 7). This will be described in more detail below (Section 3.2.4). Nevertheless, the emission spectra for excitation at 465.8 nm on samples with increasing europium content, exhibited

several peaks, assigned to $EuPO_4$ and $Ca_3Eu(PO_4)_3$ (Fig. 8). The emission line observed at 610.4 nm was recorded in all the samples irrespective of the excitation wavelength.

3.2.4. Ratio between concentration of europium ions in divalent and trivalent state

The non-selective UV excitation enabled simultaneous excitation of europium ions in the divalent and trivalent states. The ratio between the integrated Eu^{3+} and Eu^{2+} emissions as a function of the nominal content of europium in the different samples could thus be determined.

The $^5D_0$ emitting level was relatively insensitive to the multiphonon relaxation process since it was separated from the lowest $^7F_6$ multiplet by a wide energy gap. Furthermore, if the concentration in the sample is low, cross relaxation between coupled ions are unlikely to occur with Eu^{3+}. No energy transfer from Eu^{2+} to Eu^{3+} could be detected. The intensity of the intra $4f^6$ configuration $^5D_0 \rightarrow {}^7F_1$ (Eu^{3+}) dipolar magnetic transition is independent of the rare earth ion environment. Assuming the absence of non-radiative processes and interactions between ions, the $^5D_0 \rightarrow {}^7F_1$ intensity can thus be taken as a reference [17]. From the ratio between the integrated intensity of the $^5D_0 \rightarrow {}^7F_1$ (Eu^{3+}) transition and that of the Eu^{2+} emission, it is possible to derive the ratio between the relative concentrations of europium in the divalent and trivalent ionization states (Fig. 9(a)). At low concentration, europium ions were present mostly in a divalent state. The ratio between Eu^{3+} and Eu^{2+} increased with increasing europium concentration as shown on Fig. 7. The increasing ratio between europium concentration in trivalent and divalent states up to the maximum substitution level for Eu^{2+}, indicates that europium enters the lattice in a trivalent state filling the other sites as extra lines in the visible range and as $EuPO_4$ and $Ca_3Eu(PO_4)_3$ phases. This was supported by the luminescence spectra recorded under UV excitation. From Fig. 10, Eu^{3+} in $EuPO_4$ exhibits a characteristic emission line (noted as (1)). The line observed at 610.4 nm (noted as (2)) belongs to another site and is isolated from those of Eu^{3+} in the $EuPO_4$ phase. The plots of the ratio of the intensities of each of these characteristic lines with integrated emission intensity of Eu^{2+} ions is represented in Fig. 9 curves (b) and (c). It can be seen that the concentration of $EuPO_4$ increases with increase in europium content. The ratio between the emission intensity due to Eu^{3+} site at the other centre (610.3) and that of Eu^{2+} ions remained constant for different europium contents. This seems to indicate that the concentrations of Eu^{2+} and Eu^{3+} at the other site vary in the same way with increasing R_L. This means that the other site belongs to the same phase. It was ascribed to trivalent europium in the $*$ pyrophosphate phase.

Fig. 9. Ratio of Eu^{3+} fluorescence intensity taken as: ○ the $^5D_0 \rightarrow {}^7F_1$ integrated intensity, ● the intensity of line (1), ■ the intensity of line (2), with respect to Eu^{2+} integrated intensity.

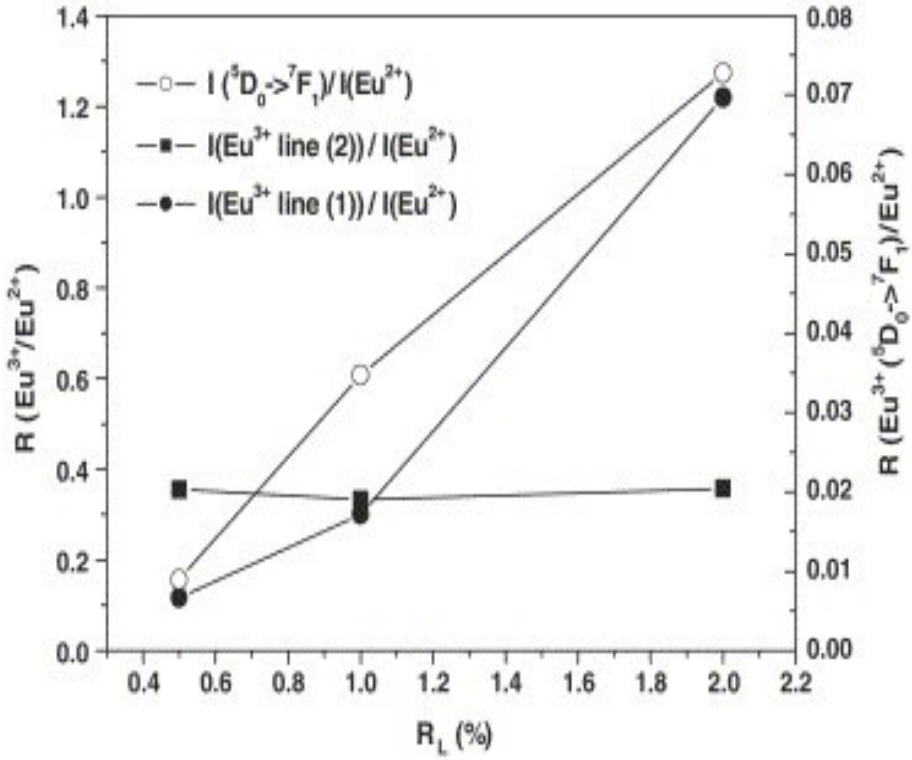

Fig. 10. Eu^{3+} luminescence spectra of the samples heated at 1270 °C recorded under UV excitation (253.7 nm) (a) R_L=0.5%; (b) R_L=1% ; (c) R_L=2% ; (d) $EuPO_4$.

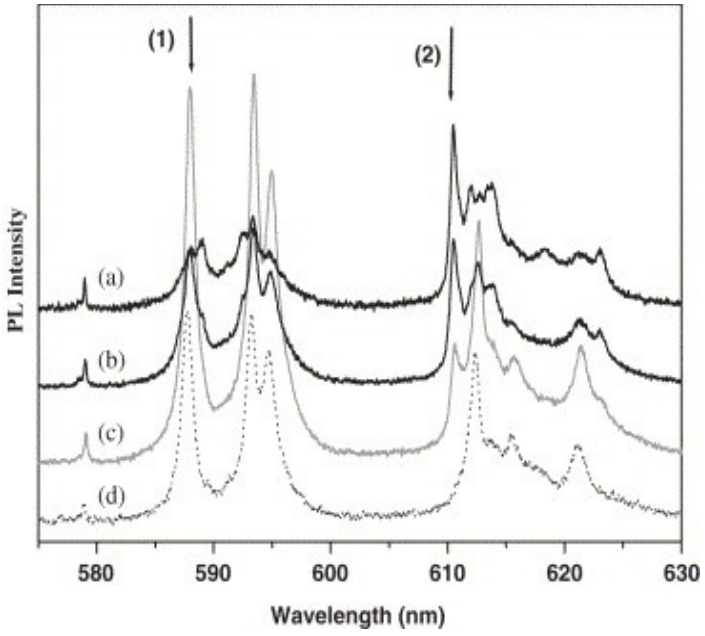

3.2.5. Spectral properties of Eu^{2+} ions

The excitation at 254 nm produced a dissymmetric wide emission band at 415 nm (Eu^{2+}), in the same position and HWHM for the samples synthesized at 1270 °C with different europium contents. Mathematical decomposition of the Eu^{2+} emission band, for the samples treated at 1250 and 1270 °C with R_L=2%, with all free parameters (peak value, bandwidth and area) produced two Gaussian curves peaking at about 23,716 cm^{-1} (421.7 nm) and 24,206 cm^{-1} (413.1 nm). Two crystallographic positions are present in ∗ pyrophosphate for calcium ions [18]. The presence of two components in the emission spectrum and their dependence on excitation wavelength stem from two different sites for Eu^{2+} ions substituting Ca^{2+} in the lattice. The relative intensity of both components to the total integrated emission spectrum calculated for the different samples was determined for the 253.7 nm excitation wavelength. The ratio between the two components calculated for samples heated at 1270 °C was not affected by europium content, whereas for the sample heated at 1250 °C, there was a greater contribution from the component peaking at 413.1 nm. For samples heated at 1270 °C during 30 min, there was an equal contribution of both components indicating that Eu^{2+} ions split uniformly between the two calcium sites on increase in temperature and time, whereas one calcium site is preferentially occupied for the samples heated at 1250 °C.

3.2.6. Excitation spectra

The excitation spectra of europium ions in the samples treated at 1270 °C were recorded. The peaks of the Eu^{2+} emission (415 nm) and the $^5D_0 \rightarrow {}^7F_1$ transition of Eu^{3+} ions (595 nm) were monitored with optimal excitation wavelenghts of 345 and 400 nm, respectively (Fig. 11). The luminescence of this sample could thus be observed in the blue or the red region of the spectrum depending on the excitation wavelength. This would represent a useful biological probe as it could be readily distinguished from other dyes.

Fig. 11. Excitation spectra of the luminescence spectrum of the sample heated at 1270 °C (R_L=2%). (a) Monitoring the Eu^{3+} emission at 595 nm; (b) monitoring the Eu^{2+} emission at 415 nm.

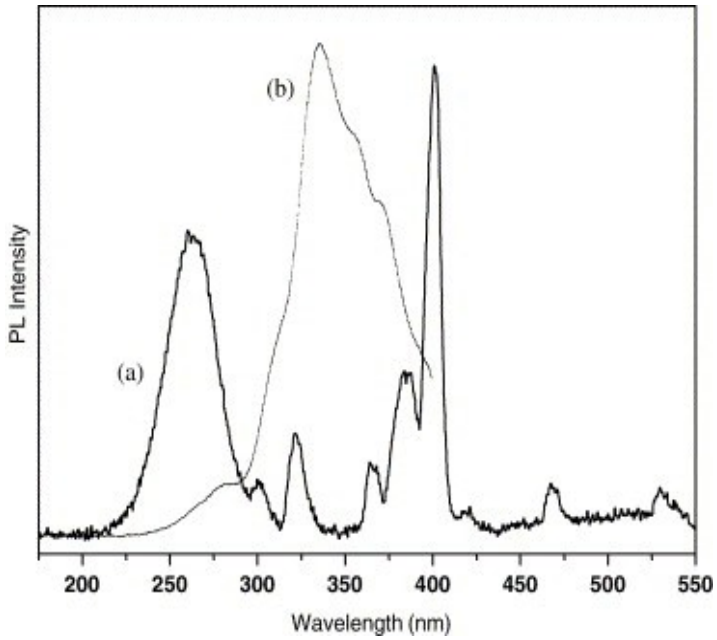

4. Discussion

Heating dicalcium phosphate samples containing europium at 900 °C leads to β calcium pyrophosphate of tetragonal structure. SEM with retro-diffused electron detection showed the existence of a small proportion of europium-rich areas. Luminescence study indicated the presence of europium phosphate $EuPO_4$ and europium-doped β tricalcium phosphate. The formation of tricalcium phosphate can be accounted for as follows: in the conditions of synthesis $Eu(OH)_3$ is formed, which on heating reacts with dicalcium phosphate $CaHPO_4$ or pyrophosphate according to the following equation:

$$3CaHPO_4+Eu(OH)_3 \rightarrow Ca_3(PO_4)_2+Eu(PO_4)+3H_2O$$

or

$$3/2Ca_2P_2O_7+Eu(OH)_3 \rightarrow Ca_3(PO_4)_2+Eu(PO_4)+3/2H_2O.$$

On heating above 1200 °C, β calcium pyrophosphate turns into monoclinic $*$ pyrophosphate. X-ray patterns and SEM with retro-diffused electron detection showed the presence of minor additional phases. They correspond to Eu-doped βTCP and $EuPO_4$. At higher temperature (1275 °C), $Ca_3Eu(PO_4)_3$ becomes stable and the following reaction takes place:

$$Ca_3(PO_4)_2+EuPO_4 \rightarrow Ca_3Eu(PO_4)_3.$$

It results in a decrease in β TCP and $EuPO_4$ depending on europium content, temperature and duration of heating.

Moreover, luminescence study indicated that divalent europium ions were located in the $*$ pyrophosphate and not in the β pyrophosphate. A partial reduction of Eu^{3+} to Eu^{2+} occurred in spite of the absence of reducing atmosphere. Eu^{2+} ions progressively occupied the two calcium sites of $*$ pyrophosphate with increase in temperature and duration of the heat treatment. Some Eu^{3+} ions however remained in the $*$ pyrophosphate structure.

These results can be explained by considering that small amounts of $EuPO_4$ are introduced in solid solution into calcium pyrophosphate during the crystallographic $\beta \rightarrow *$ transformation and due to active diffusion at this high temperature. To maintain local electroneutrality, Eu^{3+} ions are sited in the vicinity of PO_4^{3-} ions. The luminescence line at 610.4 nm observed even at low Eu content, could be assigned to Eu^{3+} ions in a particular environment within the $*$ calcium pyrophosphate phase.

This system is unstable and tends to relax, from an intracrystalline reaction, 2 PO_4^{3-} ions form $P_2O_7^{4-}$ ions:

$$2(PO_4)^{3-} \rightarrow (P_2O_7)^{4-} + 1/2O_2 + 2e^-.$$

This reaction occurs for two reasons: $P_2O_7^{4-}$ will occupy a stable conformation in the crystallographic structure of calcium pyrophosphate, and two neighbouring Eu^{3+} ions tend to be reduced into Eu^{2+}.

$$2Eu^{3+} + 2e^- \rightarrow 2Eu^{2+}.$$

In order to find out whether this abnormal reduction of Eu^{3+} to Eu^{2+} occurred in other matrixes, Eu-doped $*$ TCP was obtained by heating at 1350 °C under air, apatitic tricalcium phosphate prepared by coprecipitation in the presence of Eu^{3+} ions. Luminescence studies showed that europium remained in the trivalent oxidation state: reduction into Eu^{2+} did not take place in Eu-doped $*$ TCP. The $*$ tricalcium phosphate structure does not appear to be suitable for such reaction, indicating that the matrix plays an essential role in the reduction process under non-reducing atmosphere. Nevertheless, the presence of PO_4^{3-} ions even as a secondary phase, also appears to be required for this reaction due to their ability to condense into $P_2O_7^{4-}$ and provide electrons for the reduction of Eu^{3+}.

Finally, with increase in europium content, europium phosphate is still present as the previous reactions are only partial. This compound reacts between 1250 and 1270 °C with the previously formed β TCP leading to a mixed phosphate of eulytite structure.

5. Conclusion

We described here the different routes to europium-doped calcium pyrophosphate (from brushite) in the presence of europium ions. After heating at 1250 °C or higher, the $*$ calcium pyrophosphate phase contains both Eu^{3+} and Eu^{2+} ions. The presence of europium ions in a divalent state arises from a partial reduction of Eu^{3+} occurring at high temperature, and stabilization by the calcium pyrophosphate structure. These compounds are of particular interest as they can exhibit a red or a blue luminescence depending on the excitation wavelength. As biological probes after mechanical grinding, they could be readily distinguished from other dyes and the autofluorescence of proteins and other components of living cells by changing the excitation wavelength.

Acknowledgments

We would like to thank Mr. Thébault for the SEM observations and EDAX analysis.

References

A. Doat, M. Fanjul, F. Pellé, E. Hollande and A. Lebugle, *Biomaterials* 24 (2004), pp. 3365–3371.

J.-S. Sun, Y.C. Huang, F.-H. Lin and L.-T. Chen, *J. Biomed. Mater. Res. Part A* 64A (2003) (4), pp. 616–621.

W.L. Wanmaker and J.W. ter Vrugt, *Philips Res. Rep.* 22 (1967), pp. 355–366.

V.P. Nazarova, *Bull. Acad. Sci. USSR Phys. Ser.* (1961), pp. 322–324.

V.A. Pelova and L.S. Grigorov, *J. Lumin.* 72–74 (1997), pp. 241–243.

Q. Zeng, Z. Pei, S. Wang and Q. Su, *J. Alloy Compd.* 275–277 (1998), pp. 238–241.

Z. Pei, Q. Zeng and Q. Su, *J. Solid State Chem.* 145 (1999), pp. 212–215.

Z. Pei, Q. Zeng and Q. Su, *J. Phys. Chem. Solids* 61 (2000), pp. 9–12.

M. Peng, Z. Pei, G. Hong and Q. Su, *Chem. Phys. Lett.* 371 (2003), pp. 1–6.

Q. Su, H. Liang, T. Hu, Y. Tao and T. Liu, *J. Alloy Compd.* 344 (2002), pp. 132–136.

H. Liang, Q. Su, Y. Tao, T. Hu and T. Liu, *J. Alloy Compd.* 334 (2002), pp. 293–298.

G.J. Mc Carthy and D.E. Pfoertsch, *J. Solid State Chem.* 38 (1981) (1), pp. 128–129.

G. Charlot, Les Méthodes de la Chimie Analytique (fifth ed.), Masson, Paris (1966) pp. 658, 853.

N.C. Webb, *Acta Crystallogr.* 21 (1966), pp. 942–948.

G. Chen, J. Holsa and J.R. Peterson, *J. Phys. Chem. Solids* 58 (1997) (12), pp. 2031–2037.

B.I. Lazoriak, V.N. Golubev, R. Salmon, C. Parent and P. Hagenmuller, *Eur. J. Solid State Inorg. Chem.* 26 (1989), pp. 455–463.

C.A. Koidaira, H.F. Brito, O.L. Malta and O.A. Serra, *J. Lumin.* 101 (2003), pp. 11–21.

C. Calvo, *Inorg. Chem.* 7 (1968) (7), pp. 1345–1351

Corresponding author. Fax: +33 5 62 88 57 73.